INTERNATIONAL ATOMIC ENERGY AGENCY
UNITED NATIONS EDUCATIONAL, SCIENTIFIC AND CULTURAL ORGANIZATION

INTERNATIONAL CENTRE FOR THEORETICAL PHYSICS
34100 TRIESTE (ITALY) - P.O.B. 586 - MIRAMARE - STRADA COSTIERA 11 - TELEPHONES: 224281/2/3/4/5/6
CABLE: CENTRATOM - TELEX 460392-I

SMR/100 - 57

WINTER COLLEGE ON LASERS, ATOMIC AND MOLECULAR PHYSICS

(24 January - 25 March 1983)

Distributed Feedback Dye Lasers

A. MUELLER

Max-Planck-Institut für Biophysikalische Chemie
Am Fassberg
3400 Göttingen
FED. REP. GERMANY

DISTRIBUTED FEEDBACK DYE LASERS

Alexander Mueller
Max-Planck-Institut fuer Biophysikalische Chemie
Am Fassberg, D-3400 Goettingen

The conventional laser arrangement consists of three main elements: (1) active medium, (2) optical resonator and (3) pump source. Commonly the resonator is formed by two (or more) end mirrors providing the feedback necessary for oscillation.

In 1971 Kogelnik and Shank proposed a different arrangement in which the feedback mechanism is distributed throughout the gain medium and integrated with it. In this arrangement the feedback mechanism is provided by B r a g g s c a t t e r i n g from a periodic spatial variation of the refractive index of the gain medium, or of the gain itself.

The term "Bragg scattering" or "Bragg reflection" originates from the field of X-ray diffraction but the phenomenon is not restricted to this wavelength range. It can be observed as well with visible light or even with sound waves. We take a l a m i n a t e d g r a t i n g which consists of equidistant, partially transmitting reflective layers [FIG.1a/OHF]. A coherent light beam is coming from the left side and is partially reflected from each layer. In order to determine the directions into which maximum intensity is reflected, we can immediately get the path difference for two rays from the figure [FIG.1a]. Maxima (or minima) in the intensity of the reflected (or transmitted) wave occur when the condition $2\Lambda n \sin\vartheta = m\lambda$

is satisfied. This relationship is called B r a g g ' s l a w.
Where m = interference order.
For normal incidence ($\vartheta = 90°$) we have:

$$2n\Lambda = m\lambda$$

In order to make a DFDL we have to induce a periodic spatial variation of the refractive index n or the gain constant   of the laser medium:

$$n(z) = n + n_1 \cos Kz$$
$$\alpha(z) = \alpha + \alpha_1 \cos Kz$$

z is measured along the optic axis and $K = 2\pi/\Lambda$
Λ is the period or fringe spacing of the spatial modulation, and n_1 and α_1 are its amplitudes. A DFDL structure of this kind will then oscillate at a wavelength λ_L determined by the relationship: $\lambda_L = 2n\Lambda$

There are several ways to prepare a laser medium of this sort. The first experiments of Kogelnik and Shank used a g e l a t i n f i l m on a glass substrate. The gelatin was dichromated and exposed to the interference pattern produced by two coherent UV beams of a helium-cadmium laser [FIG.2a/OHF]. The fringe spacing in the gelatin was about $\Lambda \approx 0.3\ \mu m$
After exposure the gelatin was developed (using techniques well-known in holography) resulting in a spatial modulation of the substrate density. The developed gelatin was then immersed in a solution of r h o d a m i n e 6 G to make the dye penetrate into the porous gelatin layer. After drying the resulting DFDL structure was pumped with UV radiation from a nitrogen laser [FIG.2b/OHF]. At pump power densities $> 10^6$ W/cm^2 laser oscillation was observed at a wavelength $\lambda_L \approx 630$ nm. The linewidth was $\Delta\lambda_L < 0.5$ A (instrument limited).
When a u n i f o r m gelatin layer dyed with rhodamine 6G was pumped in the same way, stimulated emission was observed at $\lambda = 590$ nm with a line width of $\Delta\lambda \approx 50$ A. Obviously, in the first case there is considerable line narrowing due to the distributed feedback effect.

The observed behavior is due to the fact that two counterrunning waves are propagating in the periodic structure which are coupled to each other [FIG.3/OHF]. The electric field E can be expressed in the form:

$$E(z) = R(z)\exp(-jKz/2) + S(z)\exp(jKz/2)$$

where z is the direction of propagation, and R and S are complex amplitudes.
The boundary conditions are: R(-L/2) = S(L/2) = 0

At the endfaces of the device a wave starts with zero amplitude. It receives its initial energy through feedback from the other wave. The waves grow in the presence of gain and feed energy into each other due to the spatial modulation of n or α.

A DFDL structure consisting of a laser dye embedded in some polymeric matrix has the great disadvantage that it does not function for a very long period of time because all organic dyes are more or less quickly degraded by photochemical processes and in the rigid matrix they cannot be replenished. It is rather much more practical to use instead a d y e i n s o l u t i o n as the laser medium and to induce the periodic gain and refractive index variation by forming an interference pattern of the pump light on the surface of the dye cell [FIG.4a+b/].
The separation Λ of two interference maxima in this case is:

$$\Lambda = \frac{\lambda_P}{2\sin\Theta}$$

λ_P = pump wavelength

If we combine this with the Bragg condition for feedback: $\lambda_L = 2n\Lambda$
we obtain:

$$\lambda_L = \frac{n\lambda_P}{\sin\Theta}$$

The DFDL output wavelength depends on the refractive index of the dye solution n, the angle of incidence Θ of the pump light and the pumping wavelength λ_P.
Since for any chosen pumping source λ_P = const., one could either vary n or Θ for tuning the wavelength of the DFDL. But before we have a closer look at tuning let us consider still another arrangement. When you look at the last figure [FIG.4a], you will observe that rays from different parts of the pump beam are not combining with themselves to produce the interference pattern on the dye cell. That means low spatial coherence of the pump beam will result in bad fringe visibility V:

$$V = \frac{I_{max} - I_{min}}{I_{max} + I_{min}}$$

In order to improve this situation (which is necessary particularly in the case of nitrogen laser pumping) Zs. Bor (1979) proposed a scheme of the following kind [FIG.5/], in which a holographic grating is used in place of the beam splitter.
From the grating equation we have for α :

$$\sin\alpha = \lambda_p / d$$

d = spacing of the grating (mm/groove)
m = 1 (first order of diffraction assumed)

For the separation of the interference fringes we had obtained earlier:

$$\Lambda = \frac{\lambda_p}{2\sin\Theta}$$

Now consider the special case that the two mirrors are parallel, i.e. $\alpha = \Theta$. In this case it follows $\Lambda = d/2$
and

$$\lambda_L = n \cdot d$$

Because the fringe separation turns out to be independent on the pump wavelength in this case each spectral component of the pump N_2 laser creates an interference pattern with the same Λ . Therefore, we call this an a c h r o m a t i c a r r a n g e m e n t.

Additionally, if the following geometric relationship is satisfied:

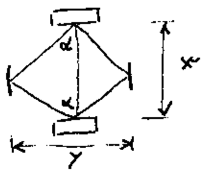

$$tg(90-\alpha) = \frac{1}{tg\alpha} = \frac{x}{y}$$

$$\frac{x}{y} = \frac{\cos\alpha}{\sin\alpha} = \frac{\sqrt{1-\sin^2\alpha}}{\sin\alpha} = \sqrt{\left(\frac{d}{\lambda_p}\right)^2 - 1}$$

for each point of the dye cell surface the two interfering beams have been diffracted from the same point on the grating ([FIG.6/OHF]: red and green lines!). Thus it is possible with this arrangement to obtain good visibility of the fringes even with a nitrogen laser which has low spatial coherence.
Note that neither of this two properties could have been obtained with the arrangement using a beam splitter in place of the grating!

The grating arrangement with parallel mirrors can be set up in a particularly compact form, which has the advantages of simplicity, stability and ease of alignment [FIG.9/DIA]. The mirrors are replaced by total internal reflections from the quartz-air interfaces of the quartz block. The next two slides [FIG.10+11/DIA] show this device in operation.

I will now turn to the methods which can be used to tune the wavelength of the DFDL:
(1) Variation of the refractive index n of the dye solution:

(1.1) Mixing of solvents with different indices n [FIG.7/OHF].

(1.2) Pressure dependence of index n [FIG.8/OHF].
The pressure dependence of n is contained in the Lorentz-Lorentz formula for the molar refraction:

$$P_M = \frac{n^2-1}{n^2+2} \cdot \frac{M}{\rho} \quad , \quad \rho = \rho(P) \quad , \quad \varkappa = \frac{1}{\rho}\left(\frac{\partial\rho}{\partial P}\right)_{T = const}$$

(tabulated) (tabulated)

Due to the low compressibility of liquids of 0.1-0.2 A/bar the tuning range is fairly small. For Pmax 100 bar the wavelength shift is $\Delta\lambda_L \sim 10 - 20$ A

(2) Another way to tune the DFDL is by changing the angle of incidence Θ which can be achieved by rotating the two mirrors in opposite directions by an angle δ about a vertical axis [FIG.12a/DIA]. In this way the fringe separation is changed:

$$\Lambda = \frac{\lambda_p}{2\sin(\Theta \pm \delta)}$$

Of course the achromatic property is lost in this case.
The lasing wavelength as a function of δ is given by [FIG.12b/DIA]:

$$\lambda_L = \frac{n\ \lambda_p}{\sin\left[\arcsin\left(\frac{\lambda_p}{d}\right) - 2\delta\right]}$$

On this basis we have recently constructed a DFDL which is continuously tunable by a computer [FIG.13a/OHF]+[FIG.13b/DIA]. The dye cell is kept stationary. The rotating mirrors and the grating are on the translation table which assures that the interference pattern remains on the dye cell surface when the angle of incidence is changed.
The next figure [FIG.14/OHF] shows tuning curves obtained with three different dyes.

(3) It is even possible to operate the DFDL in the UV and blue spectral range where the synchronously mode-locked cw dye laser does not yet work [FIG.15/OHF]. For this purpose one has to use second order Bragg reflection:

$$\lambda_L = \frac{2n\Lambda}{m} \ , \quad \text{for } m = 2 : \ \lambda_L = n\Lambda$$

for parallel mirrors:

$$\Lambda = \frac{d}{2} \ , \quad \lambda_L = \frac{nd}{2}$$

Let us now have a look at the temporal behavior of the DFDL. Together with Dr. Bor and his colleages we have investigated this problem in some detail recently.

We write down the following set of rate equations:

1) Rate of population of the upper laser level:
n = n(t), q = q(t), Ip = Ip(t) η = refractive index

$$\frac{dn}{dt} = I_p \sigma_p [N-n] - \frac{\sigma_e c}{\eta} \cdot n \cdot q - \frac{n}{\tau}$$

Pump light absorption stimulated emission spontaneous emission

2) Photon flux:
c = c(t)

$$\frac{dq}{dt} = \frac{(\sigma_e - \sigma_a)c}{\eta} \cdot n \cdot q - \frac{q}{\tau_c} + \frac{\Omega \cdot n}{\tau}$$

stimulated emission "resonator loss" amplified spont. emission (A S E)

Absorption from the upper laser level (S1) to higher excited singlet states (S1 -> Sn) is an important loss process in dye lasers that are pumped by short laser pulses. Its contribution is taken into account by including σ_a, which is implicitely also contained in τ_c (see below!).

The special features of distributed feedback are introduced with the term τ_c. In conventional lasers it describes the (constant) resonator losses. In our case a more general definition must be used since there is no external resonator in a DFDL:

$$\tau_c \sim \frac{\text{Total number of photons}}{\text{Rate of photon loss}}$$

Rate of photon loss: Output loss; Internal absorption or scattering loss; side output loss

The equivalent cavity decay time can be shown to be:

$$\tau_c(t) = \frac{\eta L^3}{2c\pi^2} \left[\alpha_1(t)\right]^2$$

we consider only the gain modulation by pumping, because it was found that the refractive index modulation makes a negligible contribution.

The amplitude of the spatial modulation of the gain is:

$$\alpha_1(t) = \sigma_e \cdot V \cdot n(t)$$

V = Visibility of fringes
n = Average population of S1

So we obtain finally

$$\tau_c(t) = \frac{\eta L^3}{8c\pi^2} \left[n(\sigma_e - \sigma_a) V\right]^2$$

This system of coupled rate equations can be solved on a small digital computer using a Runge-Kutta procedure of fourth order [FIG.16a/OHF]. The quantity which is usually most interesting is the output power of the DFDL:

$$P_{out}(t) = \frac{1}{2} \cdot \frac{hc}{\lambda_L} \cdot \frac{q(t)}{\tau_c(t)} \cdot L \cdot a \cdot b$$

a = $1/(N \cdot \sigma_p)$ penetration depth of the pump light

Now we can compare the time courses of I_P, τ_c and Pout [FIG.16b/OHF]. The diagram shows that τ_c has a strongly non-linear time dependence which gives rise to relaxation oscillations of the output. Their number depends on the pumping rate. As I will show, the pulses which are generated are of extremely short duration.
If Pout is plotted on a logarithmical scale against time one can see nicely that the intensity is changing over many orders of magnitude between the individual pulses.

In order to find out whether the system of coupled rate equations is a good model of the real DFDL we have compared results of the model computations with output pulses recorded with a streak camera system [FIG.17/DIA]. The agreement is indeed remarkably good.
A particular condition exists just below the threshold of the second pulse. Here we have a stable s i n g l e ultrashort pulse - a property of the DFDL which is very useful, and quite an advantage in comparison to mode-locked lasers where single pulse selection has to be employed using electrooptic methods.

One can now proceed to vary the various parameters of the equations and compare theoretical and experimental results quantitatively. Some examples are shown in the following figures:
[FIG.18/DIA+FIG.19/DIA+FIG.20/OHF]

Instead of temporal relationships one can just as well compare the energies of the s i n g l e pulses (cf. definition given earlier!) [FIG.21/OHF]

Since the fluorescence lifetime of the laser dye occurs in the rate equations one can try to change it by adding quenchers to the dye solution, e.g. potassium iodide KI [FIG.22/OHF]. According to the Stern-Volmer law:

$$\frac{\Phi_0}{\Phi_m} = \frac{\tau_0}{\tau_m} = 1 + k \cdot c$$

Φ_0 = fluorescence quantum yield without quencher
Φ_m = " " " with quencher
τ_0 = fluorescence lifetime without quencher
τ_m = " " with quencher

K = 68 l/mol = quenching constant

Finally one can measure the output energy of the DFDL as a function of pump power and compare it with the computed results [FIG.23/OHF], again noting that the agreement is very good.

The single pulse condition is satisfied when the DFDL is pumped about 15% above its threshold. For the computer controlled DFDL, which I presented earlier in this lecture, we have measured the single pulse condition as a function of output wavelength [FIG.24/OHF]. As a practical way to obtain single pulses we suggest the following procedure: First insert a neutral density filter with a transmission of 85% into the pump beam. Reduce the pump intensity until lasing of the DFDL stops and then remove the filter. Under these conditions single pulses will be generated most of the time.

As the figures show the duration of the single pulses is about 50 - 100 ps when a nitrogen laser having a pulse duration of 3 ns is used as the pump source. For many applications it would be desirable to generate pulses of shorter duration. If we look again at the rate equations, we see that they contain the time-dependent pumping term Ip(t). Solving them for pump pulses of shorter duration they predict a shortening of the output pulses. So we tried to construct pump lasers which would produce shorter pulses than the ones generated by the low pressure nitrogen laser used so far [FIG.25a/OHF+FIG.25b /DIA].
The electrodes of the TEA-N2-laser were connected to folded parallel plate Bluemlein lines which were switched by a hydrogen thyratron.
A telescope (M = 9) inserted between oscillator and amplifier reduced the horizontal divergence of the TEA-laser to about 1.5 mrad.
The dye bis-MSB was used as saturable absorber in the focal plane of the telescope. Repetition rate was 12 pps and 0.5 mJ were needed to pump the DFDL.

The relaxation oscillations obtained with the rate equation model are again observed experimentally. Upon lowering of the pump intensity one gets single pulses as before [FIG.26/DIA]. So, the model is well suited to describe DFDL behavior even under the conditions of variable pulse duration.
The next slide summarizes our results [FIG.27/DIA].
Each point is an average of 20 laser shots. The prediction of the rate equation model is obviously correct: Shorter pump pulses result in shorter output pulses!
From this diagram one would expect that the DFDL is capable of producing pulses as short as a few picoseconds. It is, however, obvious that the ultimate limit of pulse duration will be about one half of the transit time of light through the DFDL. Therefore, we decreased the length of the DFDL to 2mm when we used the 0.7 ns pumping pulse.
This figure [FIG.28/DIA] shows the measured pulse shape. The pulse has a FWHM of 8.8 OMA channels (OMA = optical multichannel analyzer). The sweep speed of the streak camera was 1.42+-0.02 ps/channel. Taking into account an instrumental resolution of 11 ps one can compute a pulse duration of 6 ps (FWHM).

$$\tau_{obs} = 8.8 \cdot 1.42 \text{ ps}, \quad \tau_{true} = \sqrt{\tau_{obs}^2 - \tau_{INSTR}^2} \approx 6 \text{ ps}$$

The energy of the single pulse was about 40 nJ, corresponding to a peak power of about 7 kW.

Our results show that the DFDL pulses are about 50 times shorter than the pump pulses. So, in order to find out how short are the shortest pulses we can produce, we have used pulses of 16 ps duration from a mode-locked Nd:YAG laser for pumping the DFDL.
This figure presents an outline of our setup [FIG.29/OHF]. The DFDL oscillator and the first amplifier stage are pumped with the third harmonic (353 nm) while the second amplifier stage is pumped with the second harmonic (530 nm) of the Nd:YAG laser. Since the pulses generated are too short to be measured with our streak camera, we have used a second order autocorrelation method to determine the pulse duration. The spectra of the pulses were measured simultaneously using a grating spectrograph.
We have plotted here [FIG.30/OHF] the reciprocals of the measured spectral widths ($1/\Delta\nu$) against the measured pulse durations. The experimental points lie quite well on a straight line drawn for

$$\Delta t \cdot \Delta\nu = 0.41$$

which is the time-bandwidth product of transform-limited pulses having a near-Gaussian shape as given by our model.
These are obviously the shortest pulses one can generate with a DFDL of the kind which we have used so far, their duration being limited by the transit time of light through the DFDL.

The last figure [FIG.31/OHF] summarizes the characteristics of distributed feedback lasers.

L i t e r a t u r e :

1) C.V. Shank, J.E. Bjorkholm and H. Kogelnik, Appl. Phys. Lett. [18], 395 (1971)

2) Zs. Bor, IEEE J. Quant. Electron. QE-16], 517 (1980)

3) Zs. Bor, Opt. Commun. [29], 103 (1979)

4) a) Zs. Bor, A. Mueller, B. Racz and F.P. Schaefer, Appl. Phys. [B27], 9 (1982)
   b) ibid., [B27], 77 (1982)

5) Zs. Bor, A. Mueller and B. Racz, Opt. Commun. [40], 294 (1982)

6) Zs. Bor, B. Racz and F.P. Schaefer, Kvantovaya Electron. (Moscow) [9], 1639 (1982); (Engl. Transl.: Sov. J. Quantum Electron. [12], 1050 (1982))

7) G. Szabo, A. Mueller and Zs. Bor, Appl. Phys. [B,1983] in press

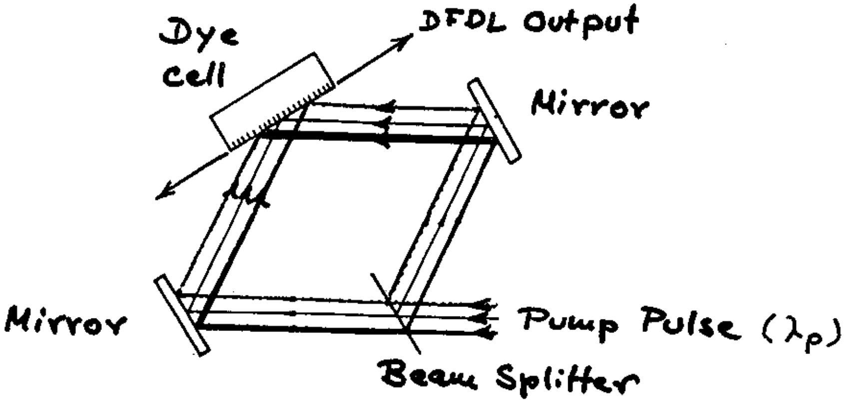

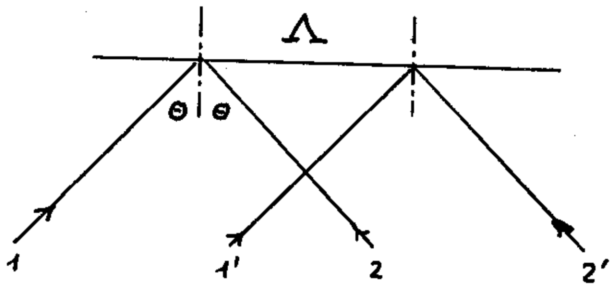

$$\Lambda = \frac{\lambda_p}{2 \sin \Theta}$$

EARLIER USED SETUP

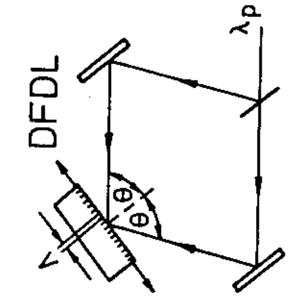

$$\Lambda = \frac{\lambda_p}{2 \sin \theta}$$

NEW SETUP

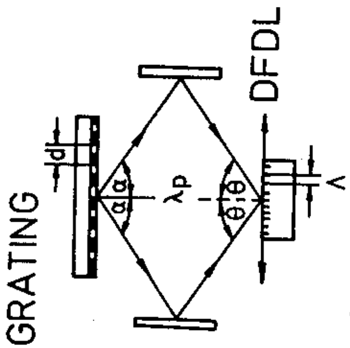

$$d \sin \alpha = \lambda_p$$

$$\frac{\lambda_p}{2 \sin \theta} = \Lambda$$

$$\alpha = \theta$$

$$\Lambda = \frac{d}{2}$$

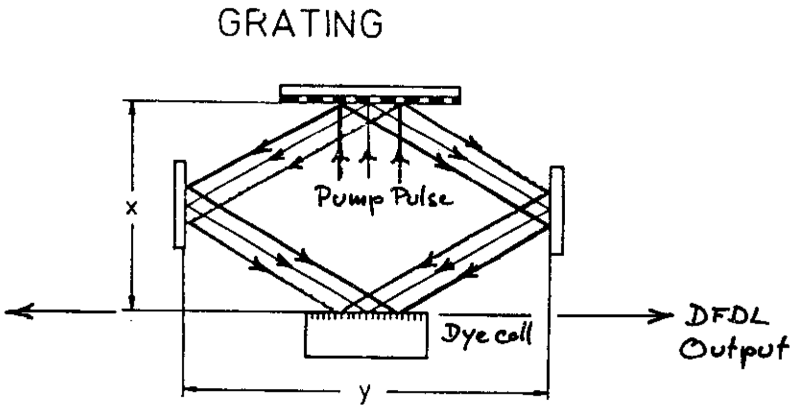
GRATING
Pump Pulse
x
y
Dye cell
DFDL
Output

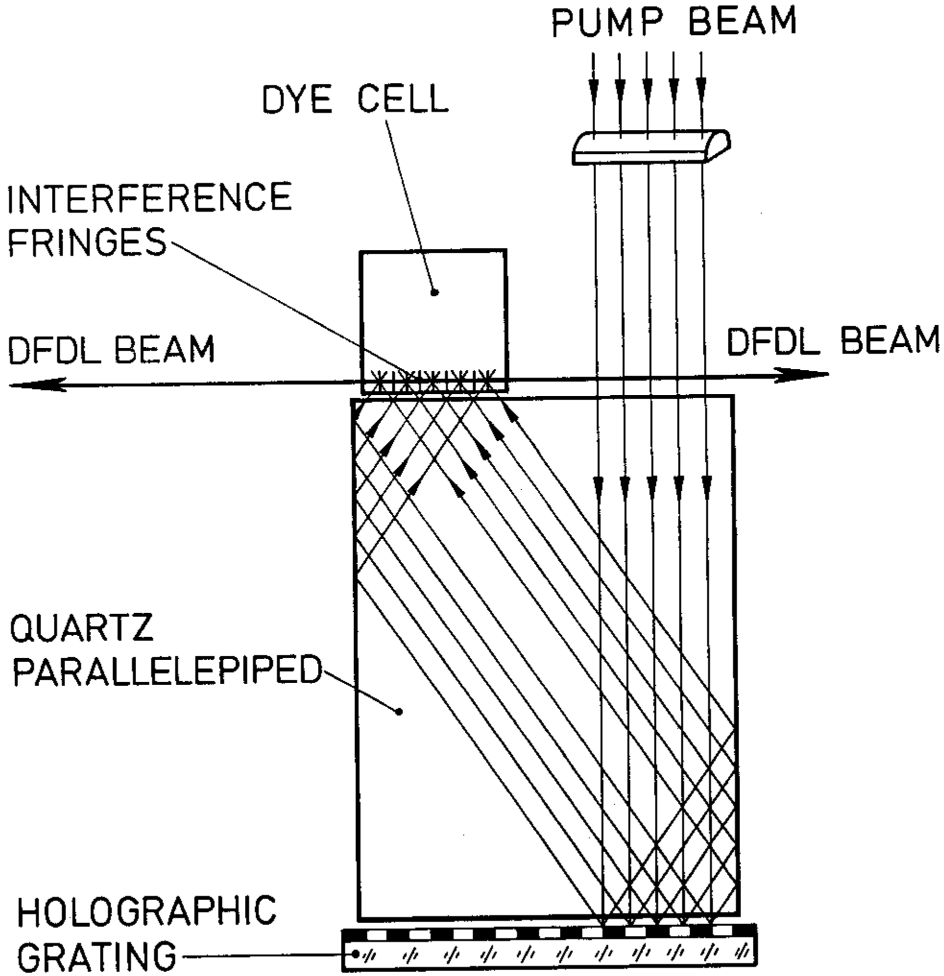
PUMP BEAM
DYE CELL
INTERFERENCE
FRINGES
DFDL BEAM
DFDL BEAM
QUARTZ
PARALLELEPIPED
HOLOGRAPHIC
GRATING

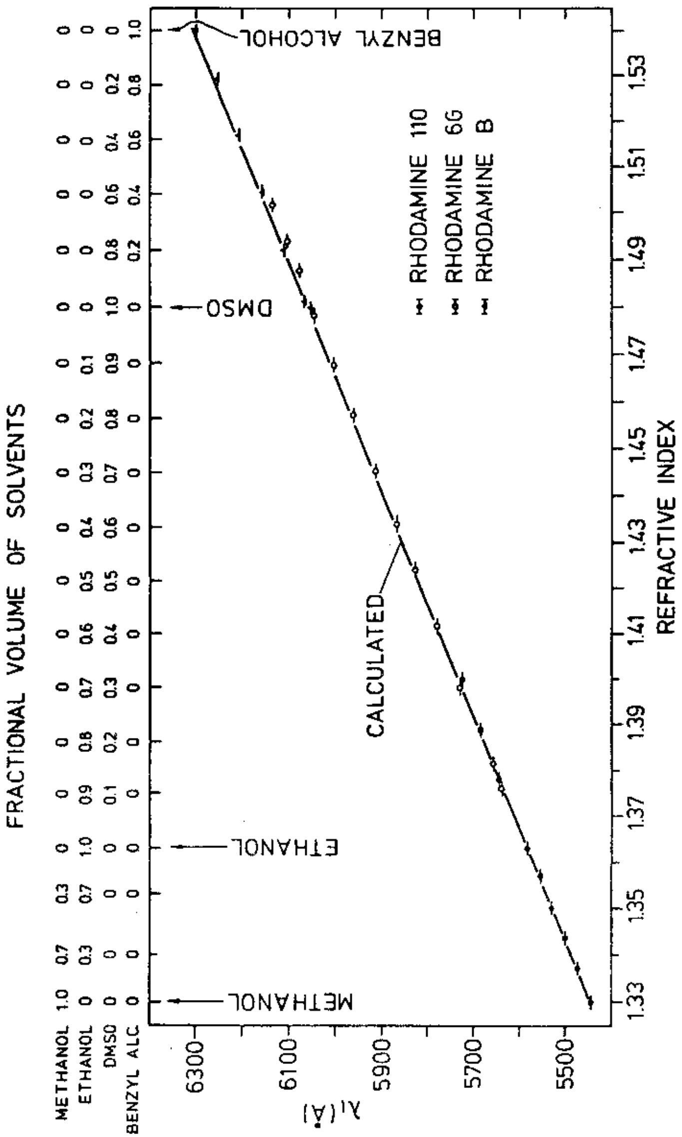
FRACTIONAL VOLUME OF SOLVENTS
METHANOL
ETHANOL
DMSO
BENZYL ALC
BENZYL ALCOHOL
DMSO
ETHANOL
METHANOL
RHODAMINE 110
RHODAMINE 6G
RHODAMINE B
CALCULATED
λ_l (Å)
REFRACTIVE INDEX

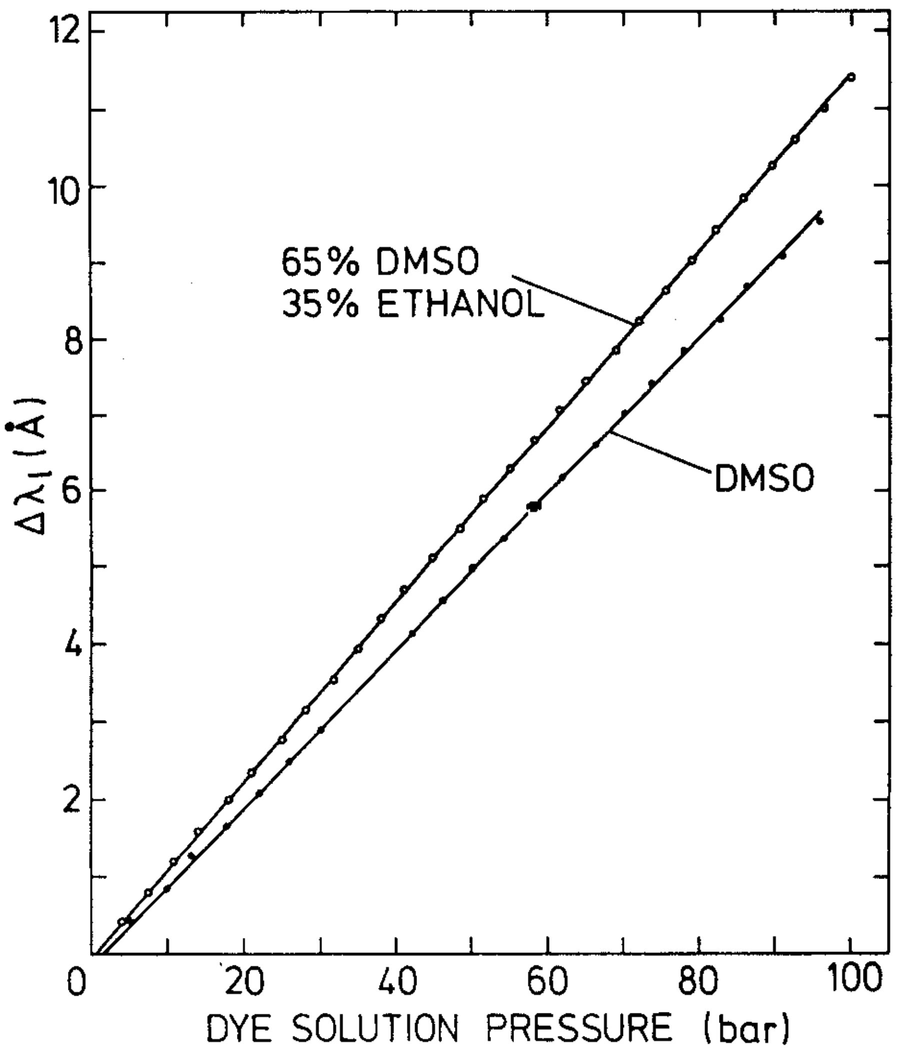
65% DMSO
35% ETHANOL
DMSO
$\Delta\lambda_l$ (Å)
DYE SOLUTION PRESSURE (bar)

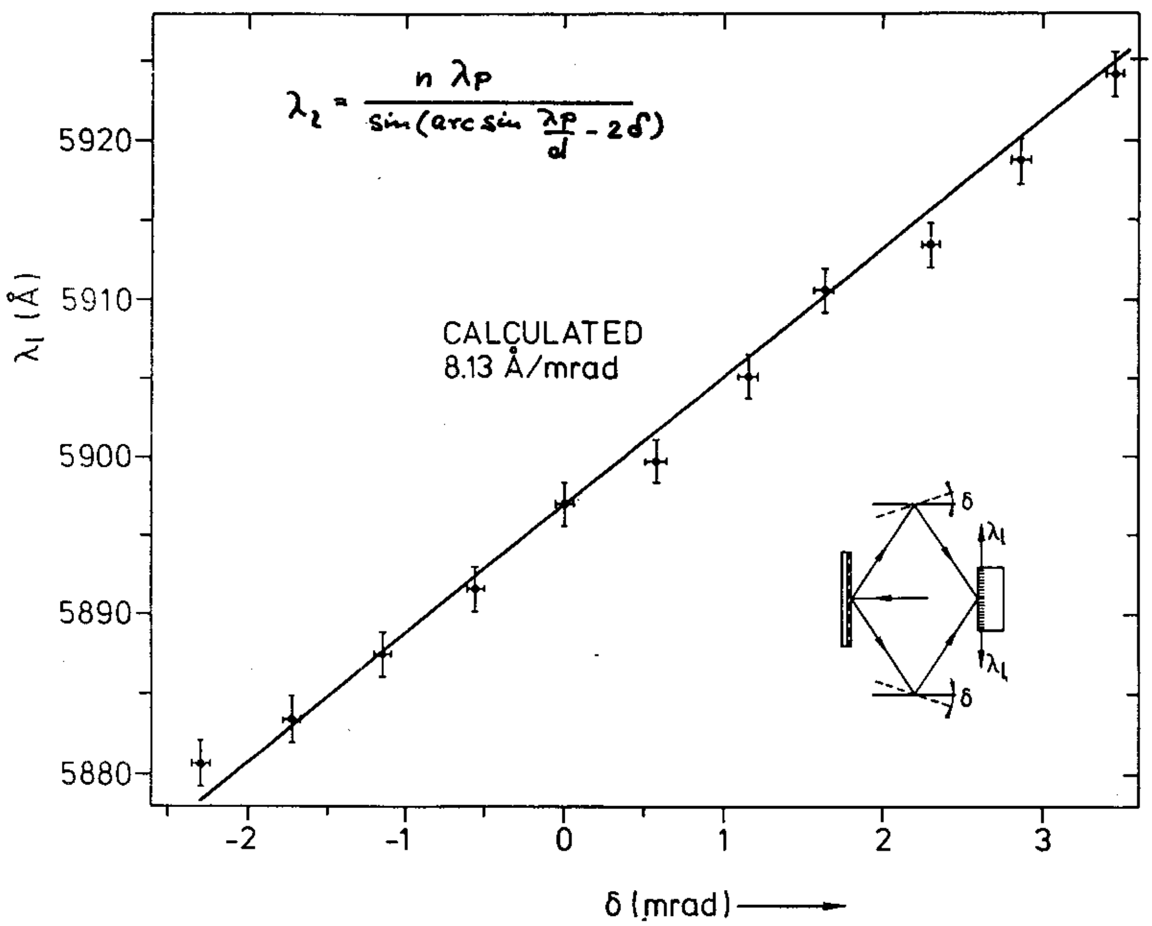

Tuning curves of computer controlled DFDL
(Single picosecond pulses)

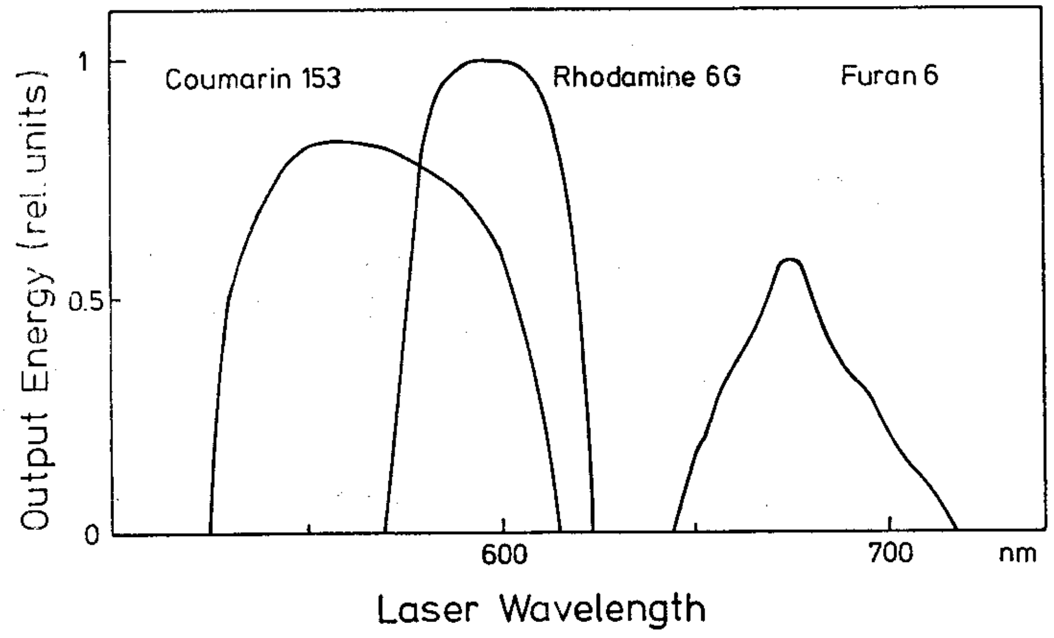

DYE	CONCENTRATION MOL/L	SOLVENT	LASING WAVELENGTH NM
PBD	$5 \cdot 10^{-3}$	38 % ETHANOL 62 % METHANOL	363
BIBUQ	$1 \cdot 10^{-3}$	80% DIOXANE 20% ETHANOL	383
BIBUQ	$1.5 \cdot 10^{-3}$	100% DIOXANE	388
DPS	$1 \cdot 10^{-3}$	90% TOLUENE 10% ETHANOL	404
STILBEN 1	SATURATED	50% DIMETHYLSULFOXIDE 50% DIPHENYLETHER	413
BIS-MSB	$1 \cdot 10^{-3}$	25% DIOXANE 75% DIPHENYLETHER	421

MODEL OF THE DFDL

$$\dot{n} = I_p \cdot \sigma_p \cdot (N - n) - \frac{\sigma_e \cdot c}{\eta} \cdot n \cdot q - \frac{n}{\tau}$$

$$\dot{q} = \frac{(\sigma_e - \sigma_a) \cdot c}{\eta} \cdot n \cdot q - \frac{q}{\tau_c} + \frac{\Omega \cdot n}{\tau}$$

$$\tau_c = \frac{\eta \cdot L^3}{8 \cdot c \cdot \pi^2} \cdot \left[n \cdot (\sigma_e - \sigma_a) \cdot V \right]^2$$

$$P_{OUT} = \frac{1}{2} \cdot \frac{h \cdot c}{\lambda_L} \cdot \frac{q}{\tau_c} \cdot L \cdot a \cdot b$$

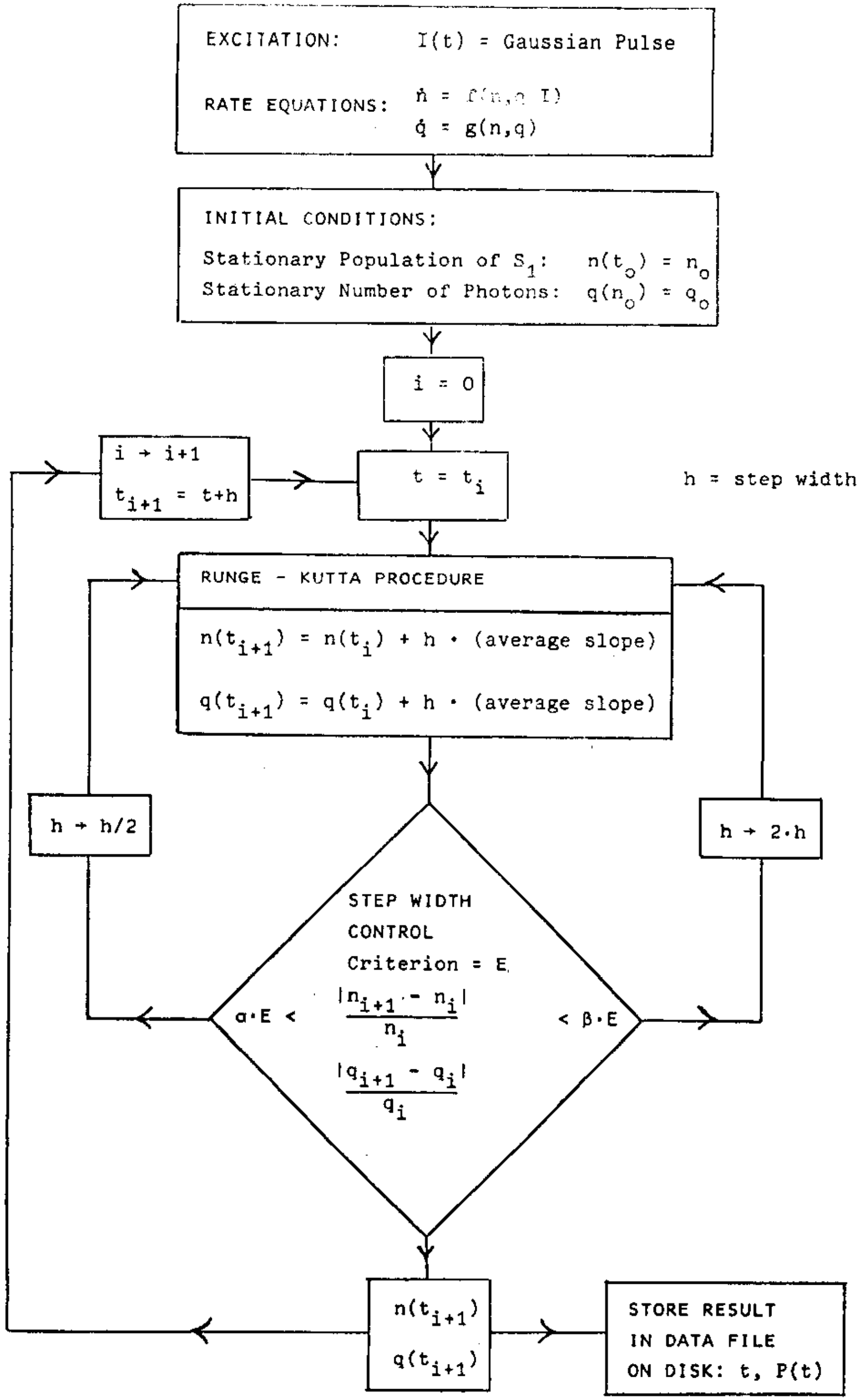
EXCITATION: I(t) = Gaussian Pulse
RATE EQUATIONS: $\dot{n} = f(n,q\ I)$
$\dot{q} = g(n,q)$
INITIAL CONDITIONS:
Stationary Population of S_1: $n(t_o) = n_o$
Stationary Number of Photons: $q(n_o) = q_o$
i = 0
$i \rightarrow i+1$
$t_{i+1} = t+h$
$t = t_i$
h = step width
RUNGE - KUTTA PROCEDURE
$n(t_{i+1}) = n(t_i) + h \cdot$ (average slope)
$q(t_{i+1}) = q(t_i) + h \cdot$ (average slope)
$h \rightarrow h/2$
$h \rightarrow 2 \cdot h$
STEP WIDTH
CONTROL
Criterion = E
$\alpha \cdot E <$
$\frac{|n_{i+1} - n_i|}{n_i}$
$\frac{|q_{i+1} - q_i|}{q_i}$
$< \beta \cdot E$
$n(t_{i+1})$
$q(t_{i+1})$
STORE RESULT
IN DATA FILE
ON DISK: t, P(t)

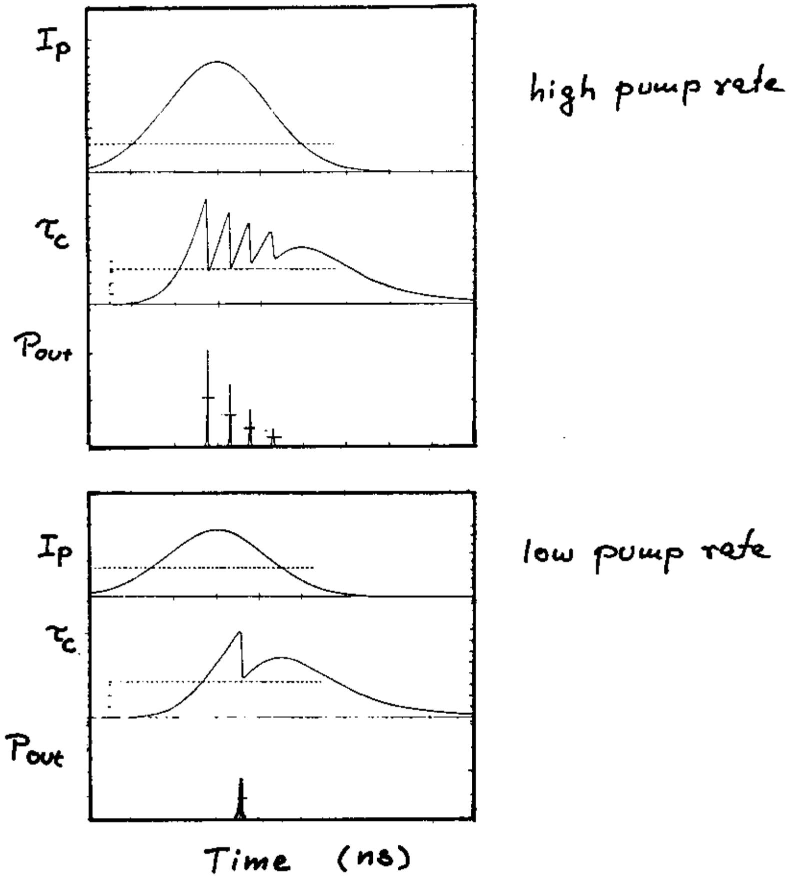
I_p
τ_c
P_{out}
high pump rate
I_p
τ_c
P_{out}
low pump rate
Time (ns)

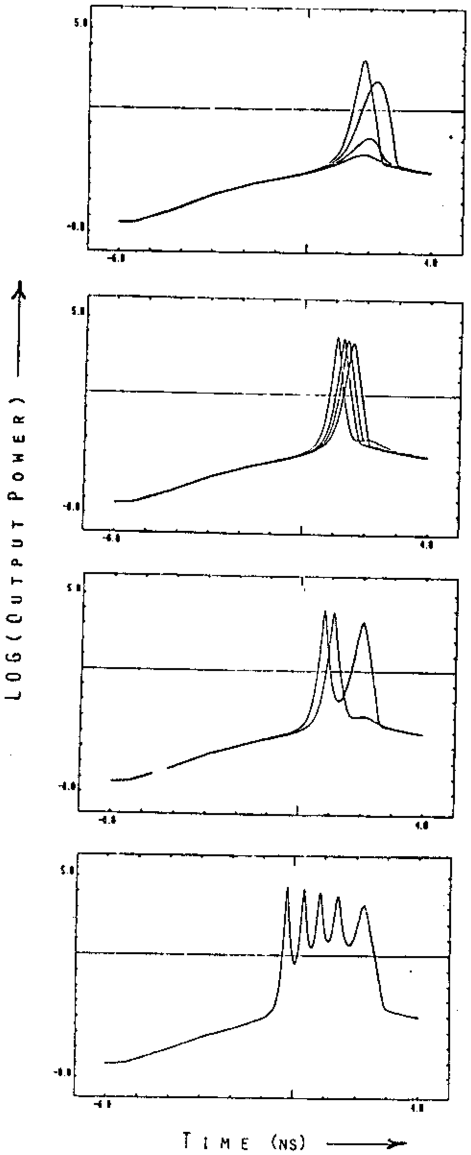
LOG(OUTPUT POWER)
TIME (NS)

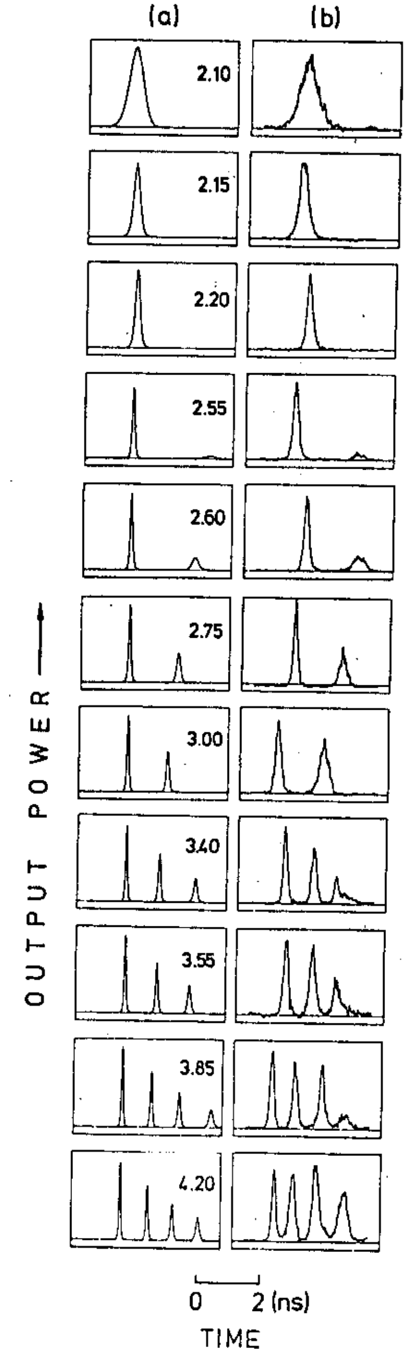
(a)
(b)
2.10
2.15
2.20
2.55
2.60
2.75
3.00
3.40
3.55
3.85
4.20
OUTPUT POWER
0
2 (ns)
TIME

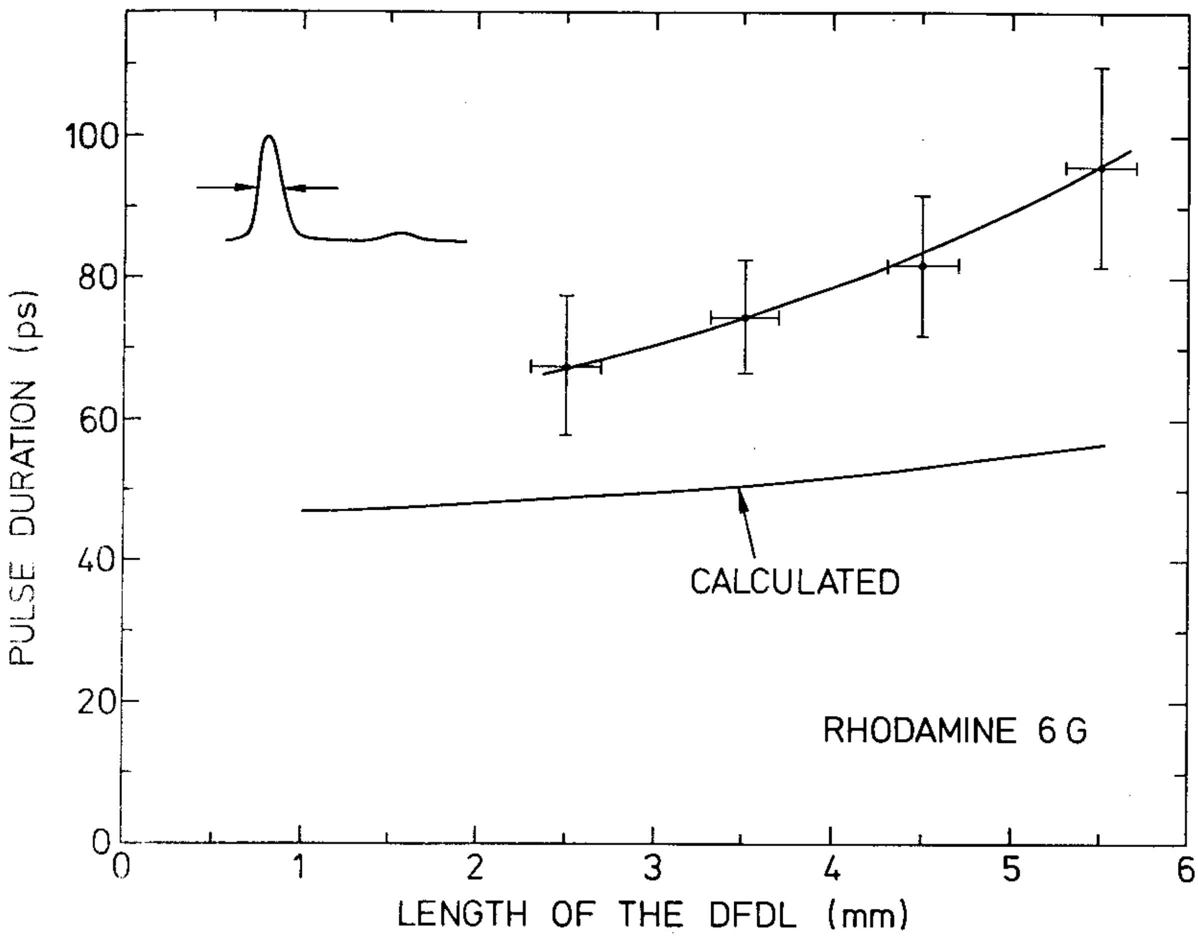

PULSE DURATION (ps)
CALCULATED
RHODAMINE 6 G
LENGTH OF THE DFDL (mm)

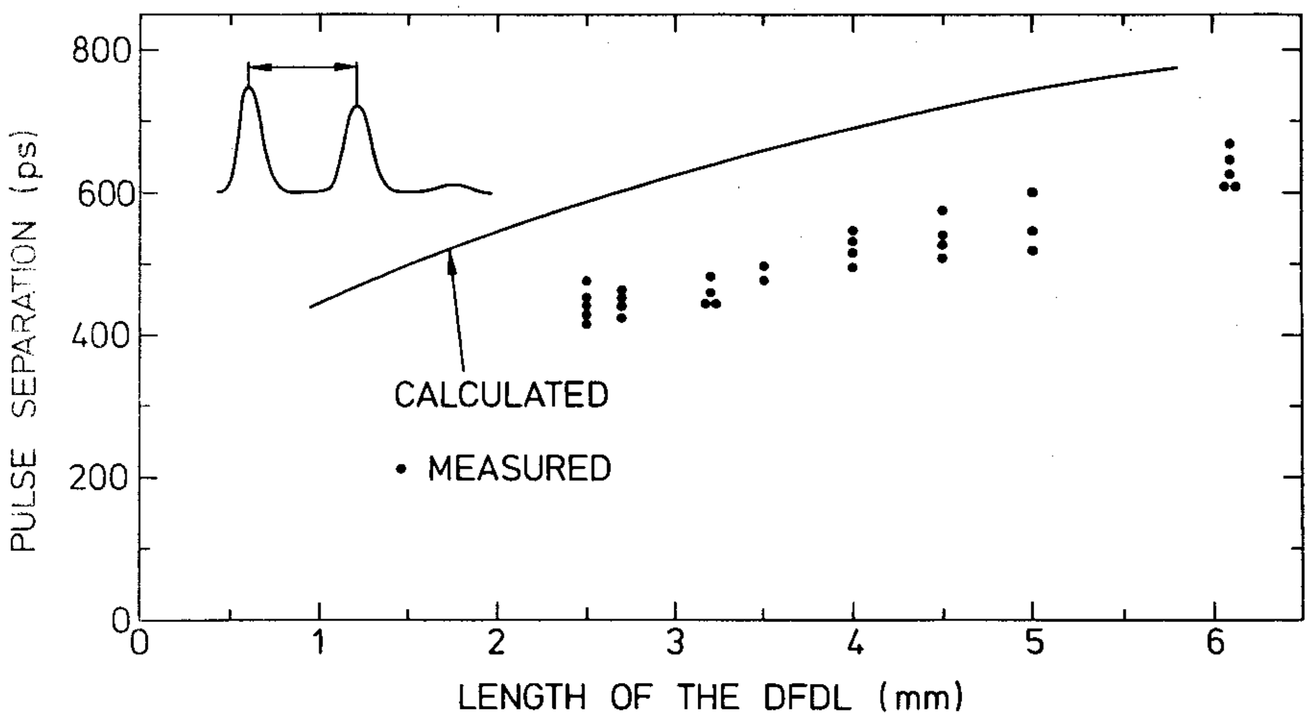

PULSE SEPARATION (ps)
CALCULATED
• MEASURED
LENGTH OF THE DFDL (mm)

(25)

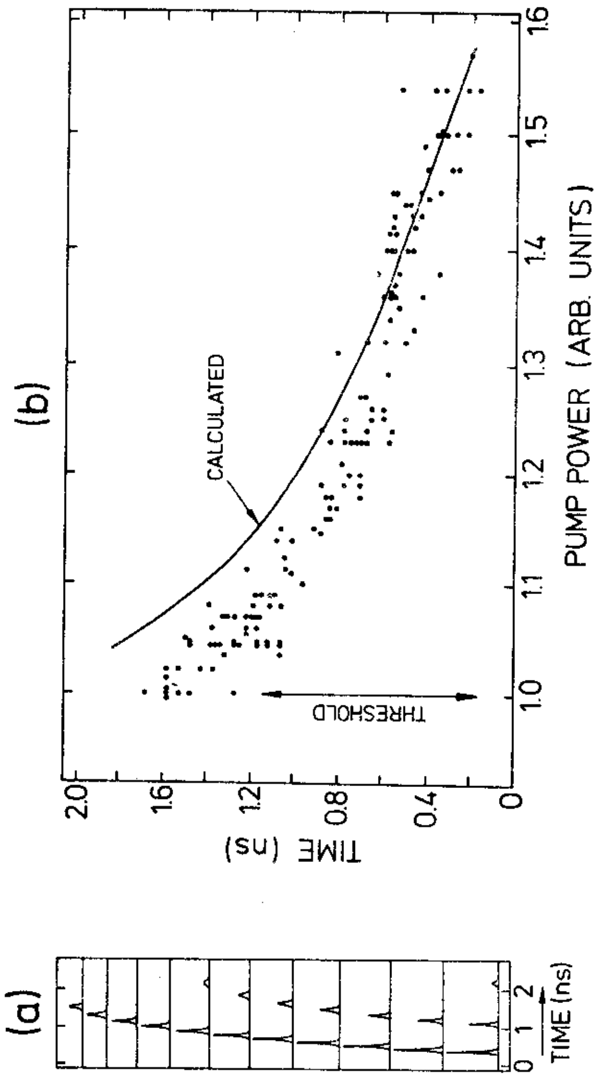
(a)
TIME (ns)
0 1 2
(b)
CALCULATED
THRESHOLD
PUMP POWER (ARB. UNITS)
1.0 1.1 1.2 1.3 1.4 1.5 1.6
TIME (ns)
2.0 1.6 1.2 0.8 0.4 0

(26)

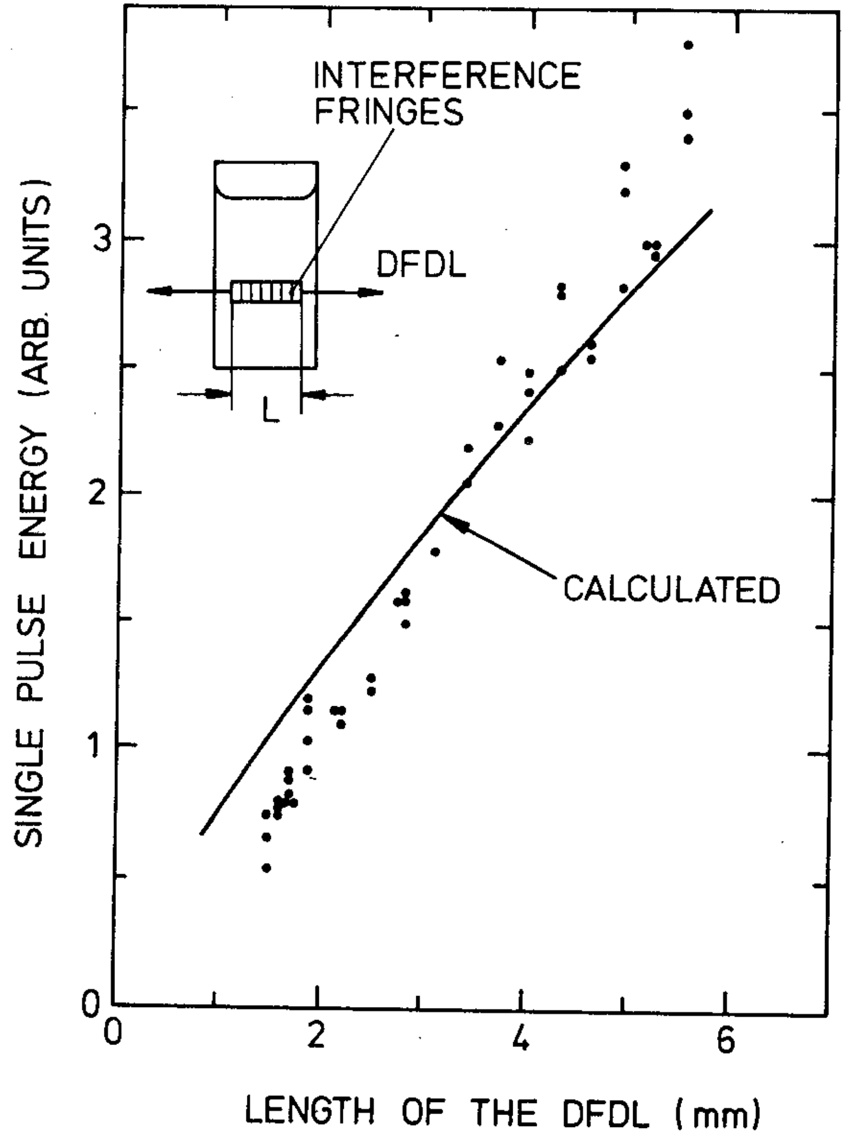
INTERFERENCE FRINGES
DFDL
L
CALCULATED
SINGLE PULSE ENERGY (ARB. UNITS)
0 1 2 3
LENGTH OF THE DFDL (mm)
0 2 4 6

(27)

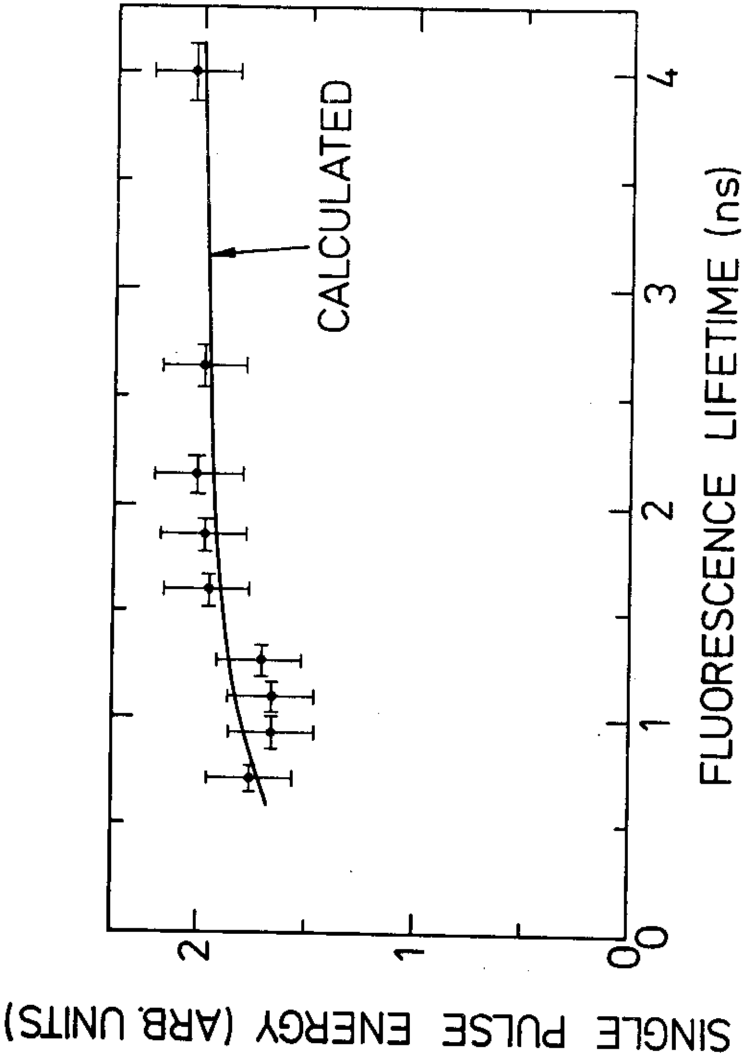
CALCULATED
FLUORESCENCE LIFETIME (ns)
SINGLE PULSE ENERGY (ARB. UNITS)
0
1
2
3
4
0
1
2

(28)

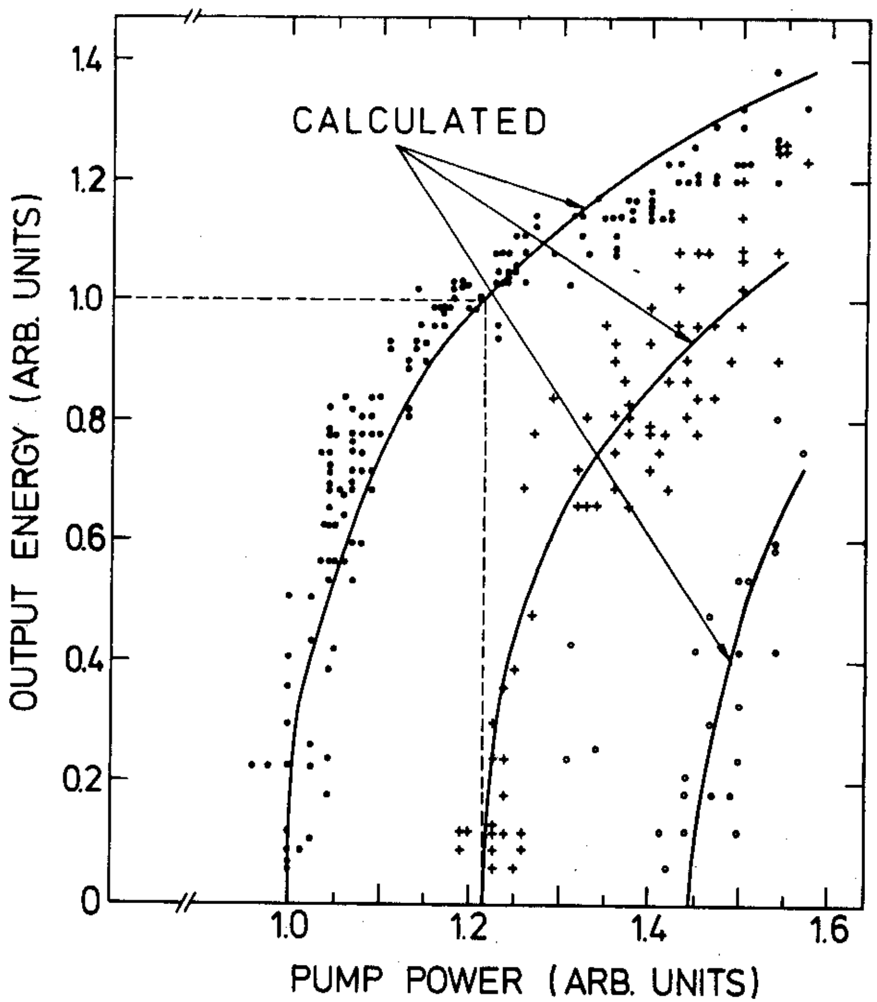
CALCULATED
OUTPUT ENERGY (ARB. UNITS)
PUMP POWER (ARB. UNITS)
0
0.2
0.4
0.6
0.8
1.0
1.2
1.4
1.0
1.2
1.4
1.6

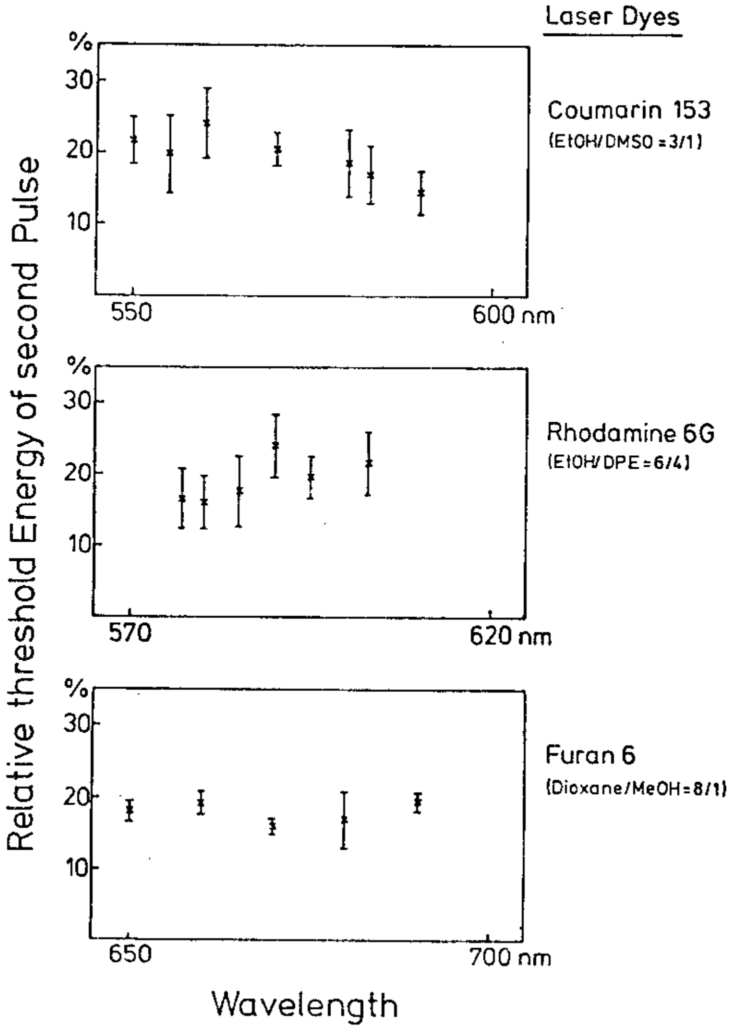

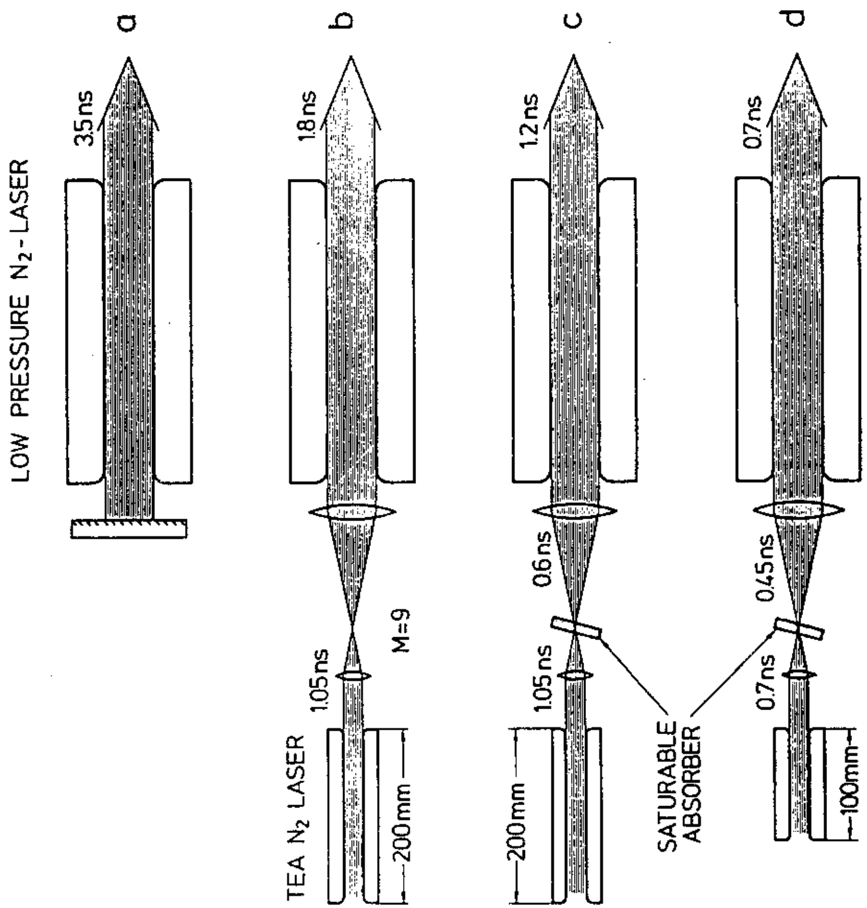

Bor/Racz/Müller:
Generation of 6-ps
pulses...
Fig. 1

Pumping Source	Pump Pulse Duration ns
Osc.: Low pressure N_2-Laser	3.5
Osc.: TEA-N_2-Laser (200 mm) Ampl.: Low pressure N_2-Laser	1.8
Osc.: TEA-N_2-Laser (200 mm) Saturable Absorber Ampl.: Low pressure N_2-Laser	1.2
Osc.: TEA-N_2-Laser (100mm) Saturable Absorber Ampl.: Low pressure N_2-Laser	0.7
Osc.: Nd : YAG (ML) Ampl.: Nd : Glass Selected single pulse Frequency tripled (354 nm)	0.016

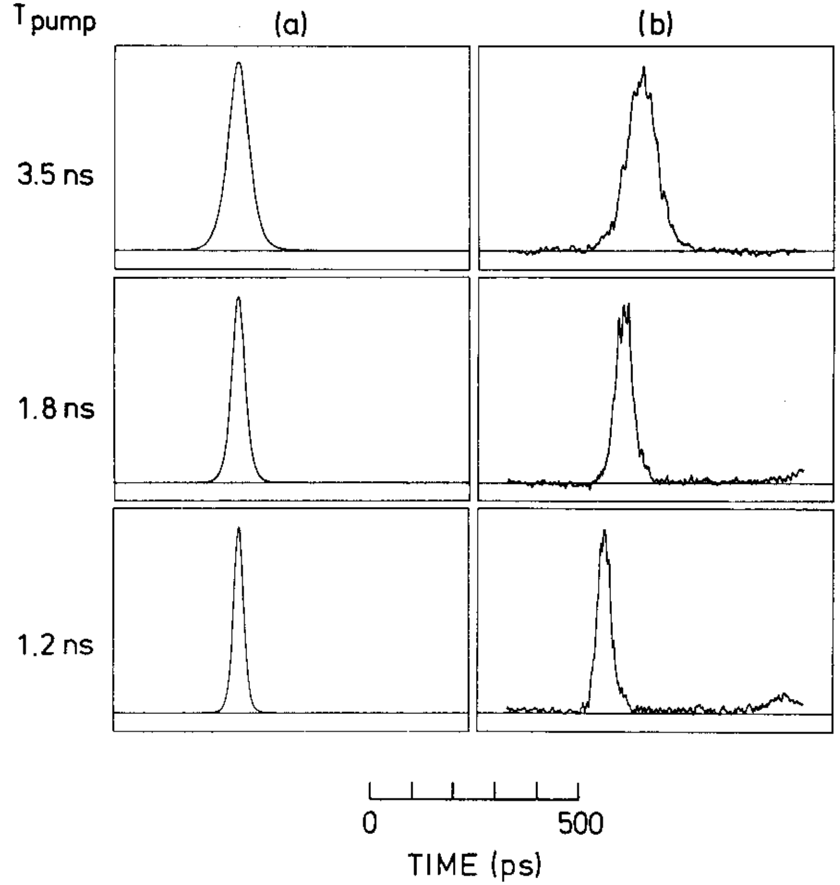

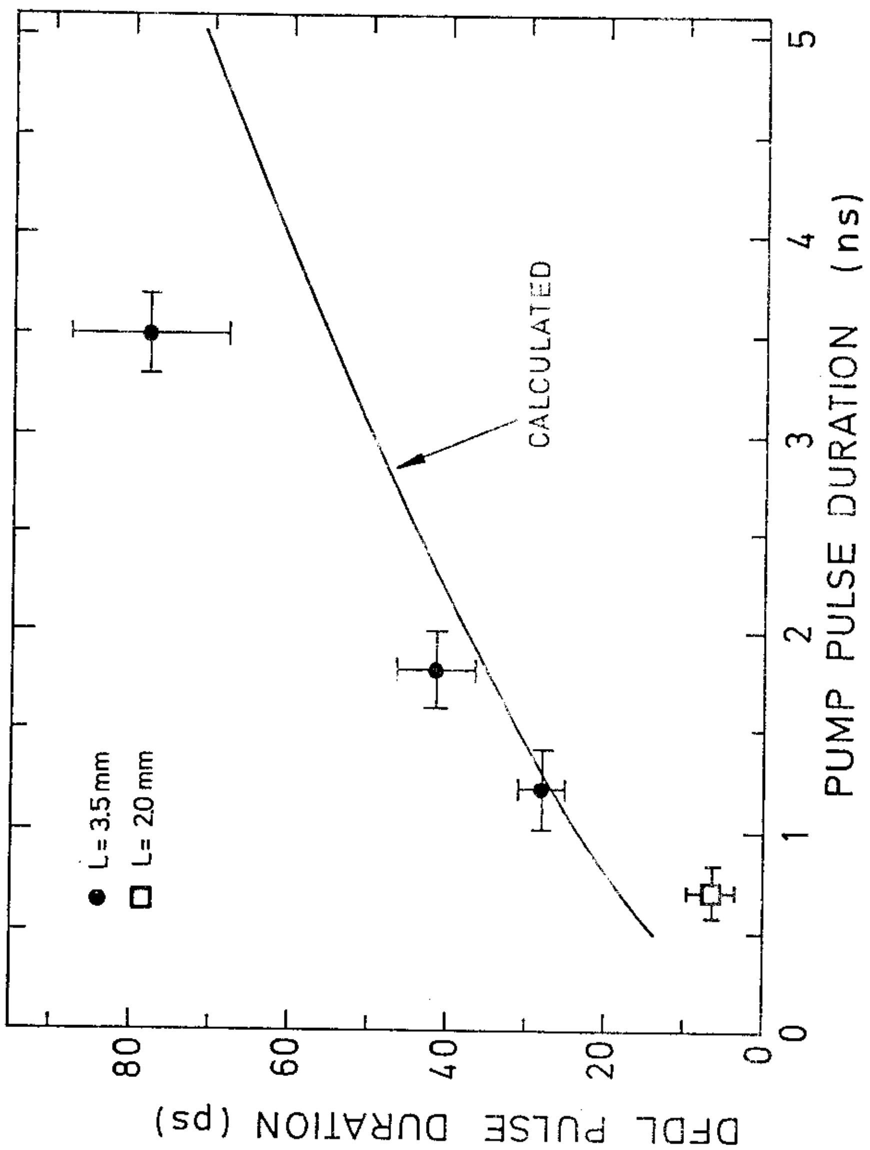

Bor/Racz/Müller:
Generation of 6-ps
pulses ...
Fig. 4

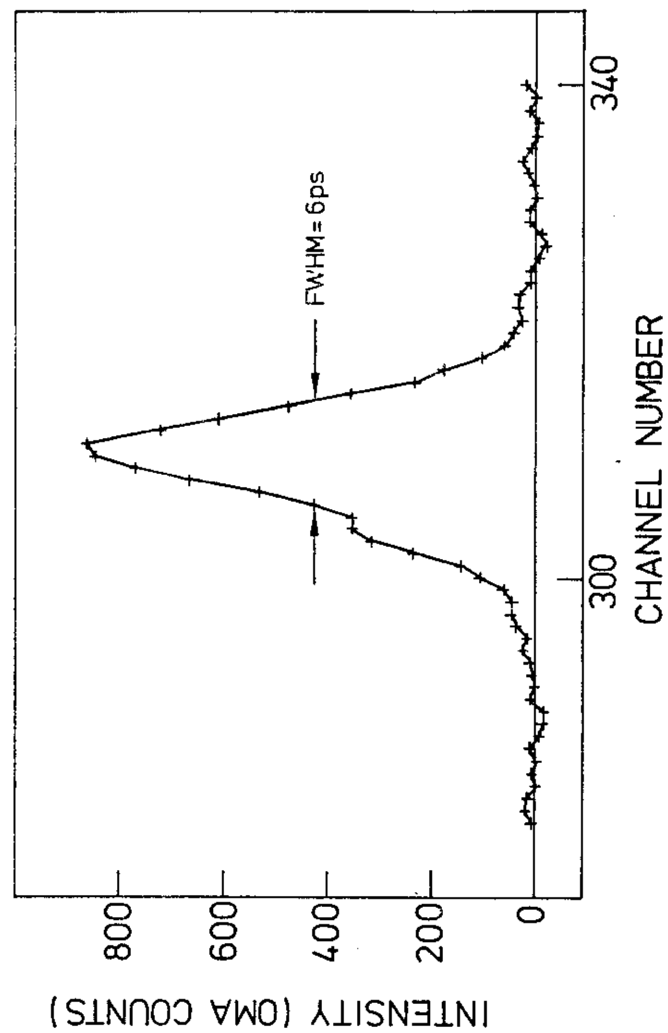

Bor/Racz/Müller:
Generation of 6-ps
pulses ...
Fig. 5

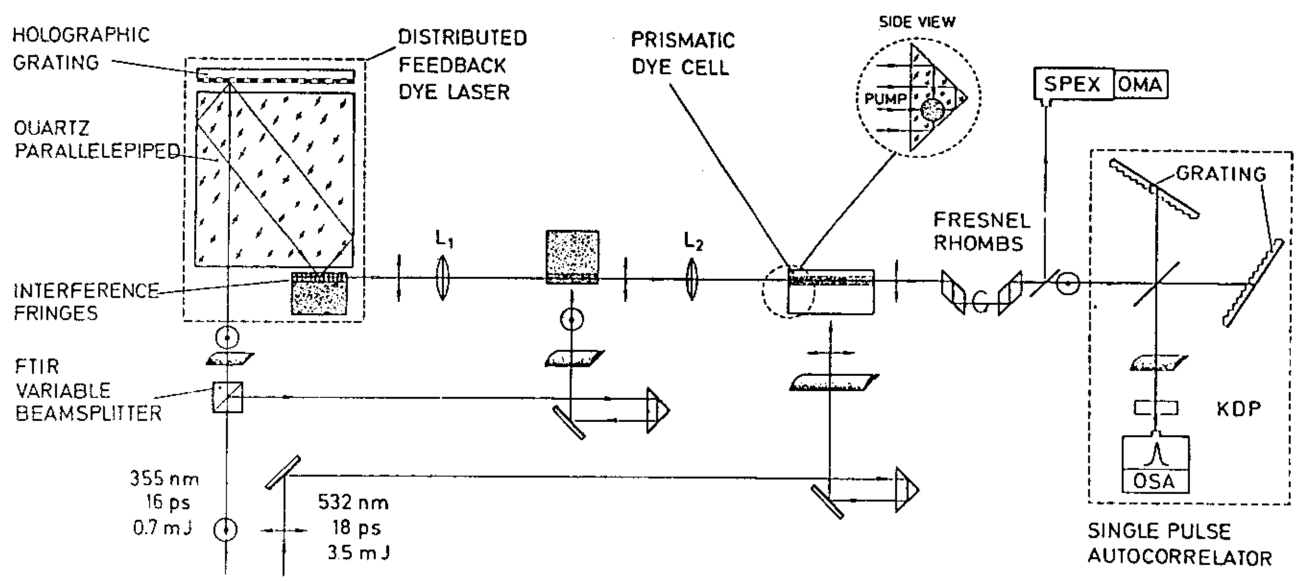

HOLOGRAPHIC
GRATING
QUARTZ
PARALLELEPIPED
INTERFERENCE
FRINGES
FTIR
VARIABLE
BEAMSPLITTER
355 nm
16 ps
0.7 mJ
532 nm
18 ps
3.5 mJ
DISTRIBUTED
FEEDBACK
DYE LASER
L1
L2
PRISMATIC
DYE CELL
SIDE VIEW
PUMP
FRESNEL
RHOMBS
SPEX
OMA
GRATING
KDP
OSA
SINGLE PULSE
AUTOCORRELATOR

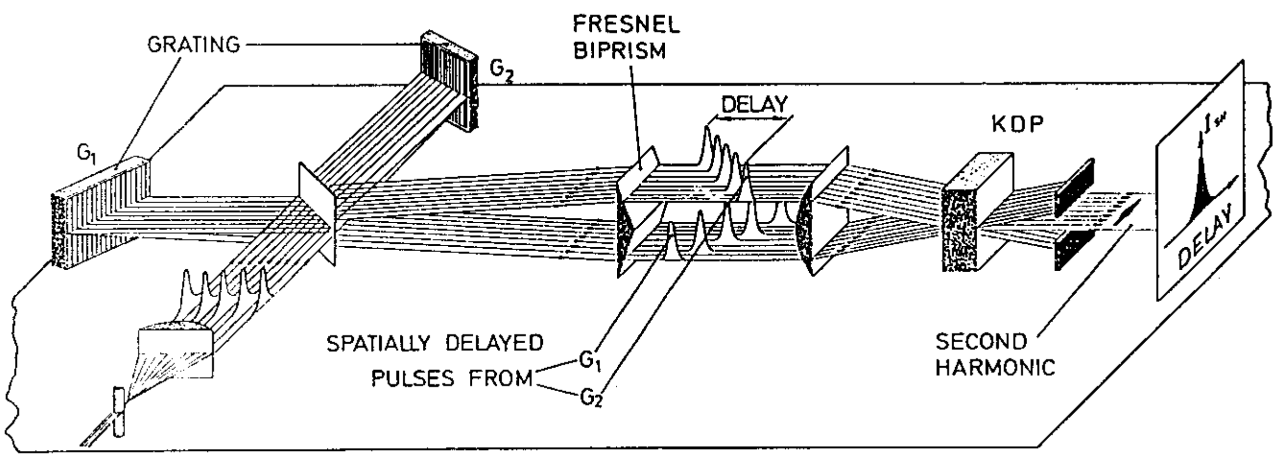

GRATING
G1
G2
FRESNEL
BIPRISM
DELAY
KDP
SPATIALLY DELAYED
PULSES FROM
G1
G2
SECOND
HARMONIC
DELAY

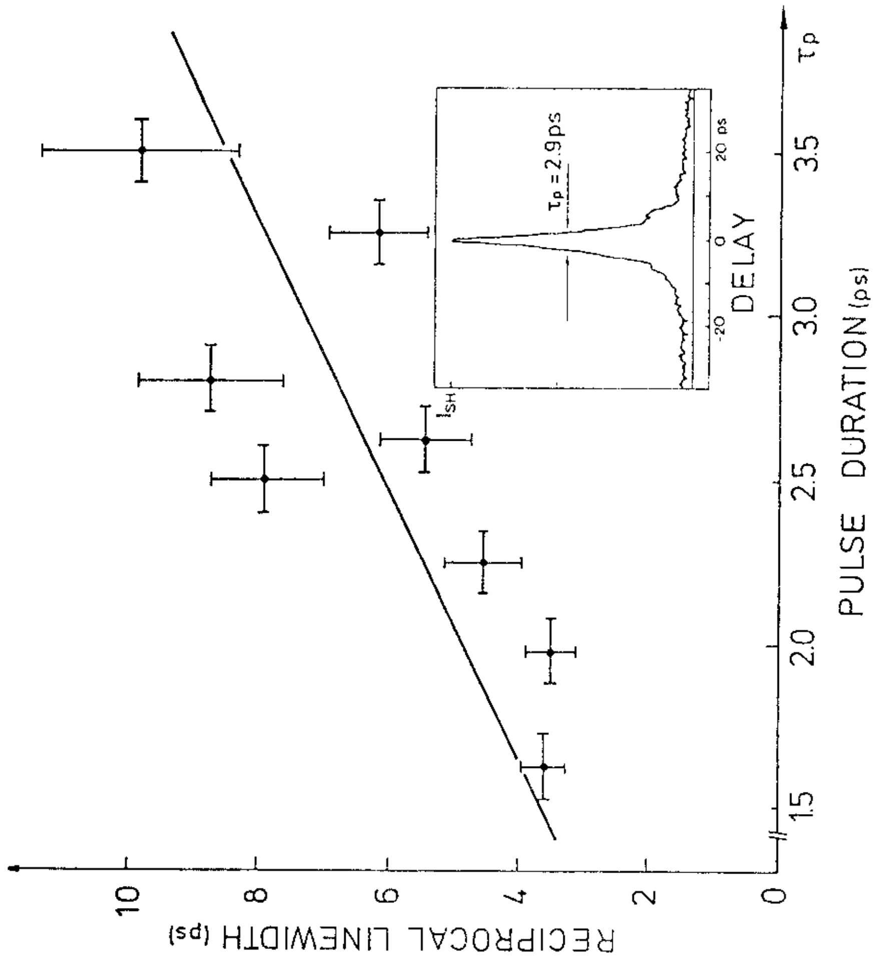

ADVANTAGES OF DISTRIBUTED FEEDBACK DYE LASERS

1. SIMPLE, RELIABLE, INEXPENSIVE.
2. SINGLE PULSES WITHOUT PULSE SELECTORS.
3. HIGH SINGLE PULSE ENERGY STABILITY /±7%/.
4. HIGH REPETITION RATE /0–200 PPS, LIMITED BY THE PUMP SOURCE/.
5. CAPABLE OF WORKING IN THE 340–1200 NM RANGE.
6. TRANSFORM LIMITED PULSES.
7. MODE-HOPPING-FREE TUNING OVER 5 NM RANGE.
8. LOWER ASE, HIGHER EFFICIENCY AND BROADER TUNING RANGE THEN THAT OF THE GRATING TUNED PULSED DYE LASERS.
9. EASY TO AMPLIFY THE PULSES UP TO 1 MW.
10. EASY TO HOME BUILT BOTH THE PUMP AND THE DYE LASER.